nature communications

Article

https://doi.org/10.1038/s41467-025-56192-3

Pupylation-based proximity labeling reveals regulatory factors in cellulose biosynthesis in Arabidopsis

Received: 4 September 2024

Accepted: 10 January 2025

Published online: 20 January 2025

Check for updates

Shuai Zheng[1], Lise C. Noack[1], Ouda Khammy[1], Andreas De Meyer[2,3], Ghazanfar Abbas Khan[4], Nancy De Winne[2,3], Dominique Eeckhout[2,3], Daniël Van Damme[2,3] & Staffan Persson[1,5]

Knowledge about how and where proteins interact provides a pillar for cell biology. Protein proximity-labeling has emerged as an important tool to detect protein interactions. Biotin-related proximity labeling approaches are by far the most commonly used but may have labeling-related drawbacks. Here, we use pupylation-based proximity labeling (PUP-IT) as a tool for protein interaction detection in plants. We show that PUP-IT readily confirmed protein interactions for several known protein complexes across different types of plant hosts and that the approach increased detection of specific interactions as compared to biotin-based proximity labeling systems. To further demonstrate the power of PUP-IT, we used the system to identify protein interactions of the protein complex that underpin cellulose synthesis in plants. Apart from known complex components, we identified the ARF-GEF BEN1 (BFA-VISUALIZED ENDOCYTIC TRAFFICKING DEFECTIVE1). We show that BEN1 contributes to cellulose synthesis by regulating both clathrin-dependent and -independent endocytosis of the cellulose synthesis protein complex from the plasma membrane. Our results highlight PUP-IT as a powerful proximity labeling system to identify protein interactions in plant cells.

Protein-protein interactions (PPIs) are at the core of all cellular processes and have the capacity to infer functions of unknown proteins. PPI analyses are done through a plethora of methods, many of which are performed in heterologous hosts or in vitro[1]. By contrast, the assessment of PPIs in native hosts is largely restricted to different affinity-based purification schemes or what is referred to as proximity labeling. Proximity labeling may be done by fusing a protein of interest, referred to as bait, with an enzyme that can label proteins in the vicinity of the bait with a certain substrate. The efficiency of this process depends on the expression level of the enzyme-tagged bait and the substrate, and on favorable conditions to catalyze the labeling. The most frequently used proximity labeling entails various versions of biotin ligases or peroxidases, including TurboID[2,3]. Some of the drawbacks of these systems include the need to add the substrate (e.g. biotin) externally, timing and temperature optimization to activate the substrate and the ability to control the labeling reaction. In addition, endogenous biotin and peroxidases may confound results in plant cells[2,3]. However, recent developments have produced a completely genetically encoded proximity labeling system using pupylation, called PUP-IT (Fig. 1a)[4].

The PUP-IT system is based on the prokaryotic enzyme PafA, which activates, holds and catalyzes the attachment of a Pup(E)

[1]Copenhagen Plant Science Center, Department of Plant & Environmental Sciences, University of Copenhagen, Frederiksberg C, Denmark. [2]Department of Plant Biotechnology and Bioinformatics, Ghent University, Ghent, Belgium. [3]VIB Center for Plant Systems Biology, Ghent, Belgium. [4]School of Life and Environmental Sciences & Centre for Sustainable Bioproducts, Deakin University, Waurn Ponds VIC, Australia. [5]Joint International Research Laboratory of Metabolic and Developmental Sciences, State Key Laboratory of Hybrid Rice, School of Life Sciences and Biotechnology, Shanghai Jiao Tong University, Shanghai, China. e-mail: Staffan.persson@plen.ku.dk

https://doi.org/10.1038/s41467-025-56192-3

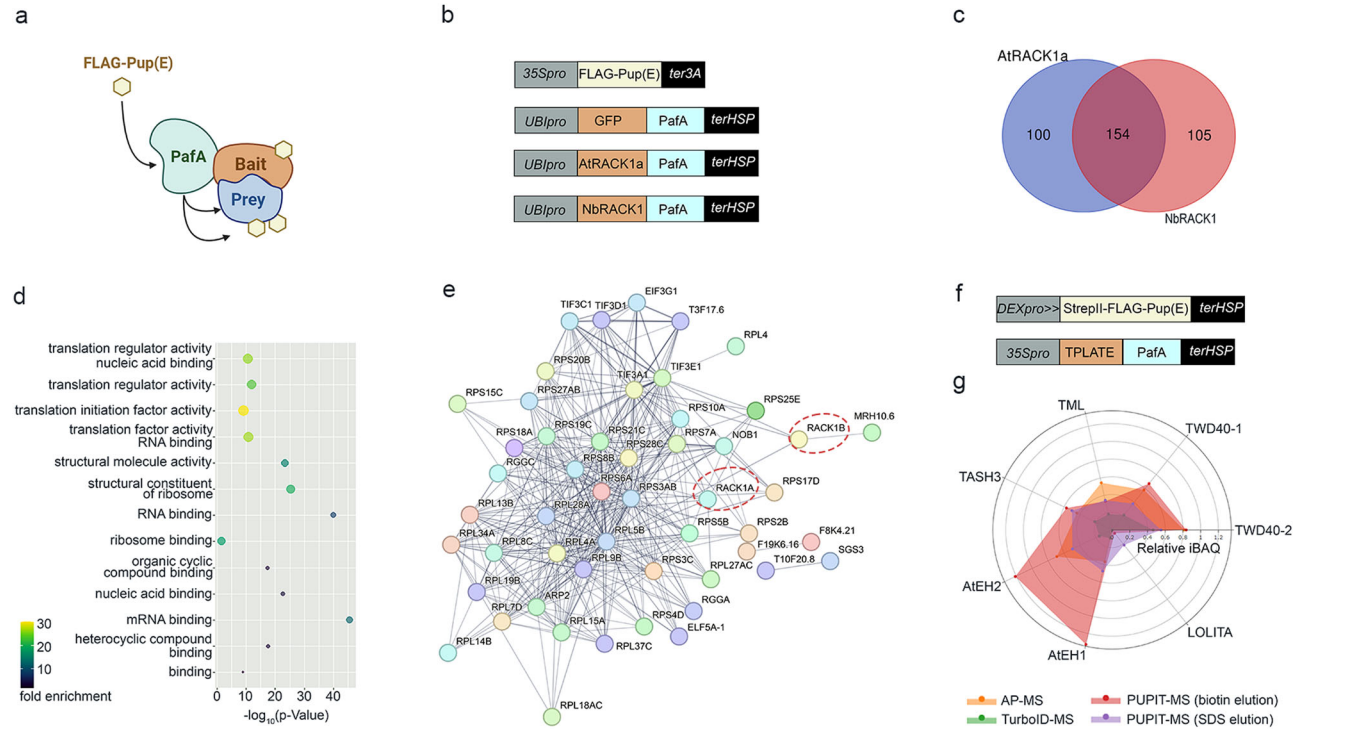

Fig. 1 | PUP-IT identifies protein interactors of RACK1 and TPLATE in plant cells. **a** Schematic of the PUP-IT proximity labeling approach [Created in BioRender. Persson, S. (2025) https://BioRender.com/z33f531]. FLAG-Pup(E) is attached to Prey protein mediated by PafA fused to a bait protein. **b** Vectors designed to express the FLAG-Pup(E) and PafA fused to GFP/AtRACK1a/NbRACK1, with cassettes for PafA and Pup(E) expressions present in one binary vector. **c** Venn diagram generated from enriched proteins of transiently expressed AtRACK1a and NbRACK1 as PafA-baits in *N. benthamiana* compared to PafA-GFP, respectively. **d** Molecular function enrichment of proteins in the overlap of (**c**). **e** A PPI network of putative RACK1 interactors that is also supported by interactions from the String database (https://string-db.org/). Nodes indicate proteins and edges indicate interactions, with line thickness indicating the strength of data support. **f** Vectors designed to express STREPII-FLAG-Pup(E) under a Dexamethasone (DEX)-inducible promoter, combined with constitutive expression of PafA fused to TPLATE. **g** iBAQ, a measure for the abundance of TPLATE subunits. iBAQ of TPLATE subunits were normalized to the bait, TPLATE, for the different experiments (as indicated below).

peptide to lysine residues of proteins in close vicinity of the PafA[4]. Pupylation is absent in eukaryotes, and thus PUP-IT may be used to label proteins without labeling background[4]. In plant science, PUP-IT has recently been used in transient protoplast assays and stable Arabidopsis lines with only one bait[5,6]. Here, we tested the PUP-IT system on a broader scale by using cytosolic and integral membrane bait proteins in a range of plant systems, including *Nicotiana benthamina* transient assays, Arabidopsis PSB-D suspension cells and *Arabidopsis thaliana* stable transgenic lines. We also added different tags on the Pup(E), e.g. FLAG-Pup(E) and StrepII-FLAG-Pup(E) providing several strategies for affinity-based protein purification of Pup(E)-tagged proteins. Finally, we provide a versatile cloning strategy with inducible- or ubiquitous promoters driving PafA and Pup(E) on the same vector backbone, which allows implementation of the system via a single transformation event.

Results

PUP-IT enables detection of known protein complexes with high specificity in plants

We first tested the PUP-IT system using the scaffold protein RECEPTOR FOR ACTIVATED C KINASE1 (RACK1) as bait in transient expression assays in *N. benthamiana* leaves. RACK1 has a plethora of interactors[7], mainly associated with protein translation and ribosome functions. RACK1 has three paralogs in Arabidopsis, of which RACK1A (AtRACK1a) is the most studied[7]. We therefore selected AtRACK1a and one of the *N. benthamiana* homologs (Supplementary Fig. 1a), referred to as NbRACK1, as baits fused to PafA in our PUP-IT approach, with GFP fused to PafA as control (Fig. 1b). We introduced a flexible linker between the PafA and the RACK1 to minimize interference of the PafA on the native bait function. We based the linker length and content (glycine-serine linkers) on the Alphafold2 predicted structure of PafA and AtRACK1 to ensure flexibility and thus functionality of the linked proteins (Supplementary Fig. 1b)[8–11]. We infiltrated the agrobacteria carrying the constructs into *N. benthamiana* leaves, performed subsequent enrichment of FLAG-Pup(E)-labeled proteins and undertook mass-spectrometry (MS) analyses to identify target proteins of the different RACK1s (Supplementary Fig. 1c–e). We next screened for proteins detected exclusively or highly enriched (t-test with false positive by permutation-based FDR = 0.05 and S0 = 1) in the RACK1-PafA samples compared to GFP-PafA (Supplementary Data 1). To compare the candidates from AtRACK1a and NtRACK1, a filter of log2(FC) > 1 was further applied. From this approach, we found 254 putative interactors of the AtRACK1a and 259 of the NbRACK1 compared to the GFP control (Fig. 1c; Supplementary Data 1). Importantly, we found that 154 of these proteins overlapped between the AtRACK1a and NbRACK1 samples (Fig. 1c), corroborating our expectation that the RACK1s in Arabidopsis and *N. benthamiana* engage with similar proteomes. To assess what processes were enriched among these proteins we next undertook Gene Ontology (GO) analyses and found that terms related to protein translation, RNA binding and ribosome function were among the most enriched for the proteins in line with the known activity of RACK1 (Fig. 1d). To further corroborate these inferences, we looked at overlap between the PUP-IT identified interactors and known interactors. To do this, we identified Arabidopsis homologs of the potential RACK1 interactors from the *N. benthamiana* PUP-IT experiment using BLAST and selected the best score hits. We then used these homologs to search the RACK1 interactome via the STRING database (https://string-db.org/). Out of the 154 proteins enriched from our

RACK1 experiments, we found 51 proteins closely connected to RACK1 in STRING (Fig. 1e, network type: physical subnetwork, active interaction sources: experiments). In addition, several other interacting proteins formed smaller connected satellite units. It is important to note that although the BLAST analyses may have identified true orthologs between Arabidopsis and *N. benthamiana*, it is also possible that some proteins are part of more complex protein families, which may lead to an underestimation of positive hits.

We next tested the PUP-IT approach in another commonly used system for proteomics in plant biology, Arabidopsis PSB-D suspension cells. Here, we chose to investigate the TPLATE complex (TPC), which is a key endocytic protein complex in plant cells containing eight subunits[12]. We, therefore, fused the PafA with TPLATE via a GSL linker and combined it with the expression of StrepII-FLAG-Pup(E) under a dexamethasone (DEX)-inducible promoter on the same T-DNA (Fig. 1f). We first optimized the time points and concentrations of DEX treatment by detecting the StrepII-FLAG-Pup(E) labeled TPLATE bait (Supplementary Fig. 2a, b). Next, we affinity-purified the pupylated proteins and probed the bead fractions with an antibody against AtEH1/Pan1, a subunit of the TPC. The co-purification of the AtEH1/Pan1 subunit served as a first proxy for complex incorporation of the tagged bait (Supplementary Fig. 2c). We also tested whether we could elute the majority of StrepII-FLAG-Pup(E) labeled proteins with 50 mM biotin while minimizing Streptactin contamination, which could interfere with mass spectrometry analysis (Supplementary Fig. 2d). In parallel with the biotin elution strategy, we also used an SDS elution procedure (Supplementary Fig. 2e). From the samples treated with DEX compared to mock as control, proteomic analyses showed that PUP-IT has the capacity to specifically isolate the TPLATE complex as various subunits of the TPLATE complex were significantly enriched or even exclusively found in the DEX group (Supplementary Fig. 2f, g; Supplementary Data 2). Furthermore, the absence of the FLAG-Pup(E) peptides in the control group indicates that the DEX-inducible system in PSB-D is not leaky and therefore allowed tight control over the reaction (Supplementary Fig. 2f, g; Supplementary Data 2). Affinity Purification-Mass Spectrometry (AP-MS) and TurboID-based biotin-proximity labeling have previously been performed on TPLATE in the same system, which allowed us to compare PUP-IT to these approaches[12,13]. To do this, we undertook intensity-based absolute quantification (iBAQ)[14] of TPLATE subunits normalized to TPLATE as measure of enrichment of the subunits for each of the different experiments. We found that the subunits were substantially more enriched in the PUP-IT-based approaches compared to both AP-MS and the TurboID assays, highlighting high specificity of PUP-IT in labeling known TPLATE interactors (Fig. 1g; Supplementary Data 2).

Implementation of PUP-IT in stable transgenic Arabidopsis lines identifies cellulose synthesis-related proteins

The above examples demonstrate the utility of PUP-IT as an effective proximity labeling system in plant biology. We next employed the PUP-IT system to investigate the membrane-based CELLULOSE SYNTHASE (CESA) complex (CSC), which underpins cellulose synthesis in plant cell wall biology[15]. CSC has many known interactors; however, mechanisms that regulate CESA activity and trafficking are still unclear, suggesting that we are missing important interactors. Here, we chose to fuse the PafA to the N-terminus of COMPANION OF CESA 1 (CC1) (Supplementary Fig. 3a), which is one of the central components of the CSC[16] and transformed the construct either into *N. benthamiana* leaf cells (transient infiltration) or into *cc1cc2* double mutant Arabidopsis plants (stable transformation). As the CSC is largely present at the plasma membrane, we used the plasma membrane-localized protein LOW TEMPERATURE INDUCED PROTEIN 6B (LTI6B) as control (Supplementary Fig. 3a). We first analyzed the enriched proteins from the *N. benthamiana* infiltration and found that many of the known CESA complex proteins were enriched in the CC1 samples as compared to the LTI6B (Fig. 2a; Supplementary Fig. 3b, c; Supplementary Data 3). For example, beyond CC1, we found *N. benthamiana* proteins corresponding to the main CESAs that make up the core of the complex (e.g. CESA1), as well as CESA INTERACTING1 (CSI1) that connects the CSC to underlying microtubules[17]. In addition, we found SHOU4-LIKE that regulates trafficking of the CSC, as well as the STRUBBELIG-RECEPTOR FAMILY6 (SRF6) that is involved in response to cellulose deficiency (Fig. 2a; Supplementary Data 3)[18,19].

With these promising results, we next generated Arabidopsis stable transgenic lines using either a *CC1* promoter- or *Ubiquitin10* promoter (UBI10pro)-driven PafA-CC1 construct to transform *cc1cc2* double mutant plants. We used plants expressing a UBI10pro-driven PafA-LTI6B construct as control. We screened independent transgenic lines to obtain suitable levels of PafA-LTI6B and PafA-CC1 activity, and then selected lines based on the ability of the PafA-CC1 to complement the *cc1cc2* mutant phenotype (Supplementary Fig. 3d–f). Here, we scored the phenotype based on growth on media plates supplemented with the cellulose synthesis inhibitor isoxaben, which leads to severe growth retardation of *cc1cc2* mutant roots[16]. We found that while the CC1 promoter-driven constructs partially complemented the isoxaben-related phenotypes of *cc1cc2*, the UBI10pro-driven constructs complemented the phenotypes better (Supplementary Fig. 3g, h). Based on these results, and since we used the UBI10pro-driven LTI6b expression as control, we chose to use the UBI10pro-driven PafA-CC1 expression for our PUP-IT experiments. To ensure that we both had sufficient material for enrichment assays, as well as active cellulose synthesis, we used six-day-old seedlings as material for the FLAG-Pup(E) enrichment (Supplementary Fig. 3i). Similar to the transient infiltration assays in *N. benthamiana* leaves, we again found the components of the core cellulose synthesis machinery including CESAs (1, 3 and 6) and CSI (1 and 3)[20], as well the SHOU4, SRF1 corresponding to their homologs SHOU4L and SRF6 identified in the *N. benthamiana* samples (Fig. 2a, b; Supplementary Data 4). In addition, we found the subunits of TPLATE complex, which mediates CSC endocytosis, as well as the v-ATPase subunit DE-ETIOLATED3 (DET3) involved in CSC secretion and recycling at the *trans*-Golgi network (TGN)[21,22]. We note that despite using different organisms, conditions, transformation approaches and organs, we identified the key core proteins of the CSC using the PafA-CC1 in *N. benthamiana* and Arabidopsis. However, the CC1 interactomes differ across the comparison, possibly indicating that the interactomes of a given protein vary depending on development, environment and biological system.

BEN1 interacts with the N-terminal domain of CC1

While some of the components of the CSC have been identified based on forward genetic screens, many of the more recently identified components have been found via co-expression analyses[23]. To see if any of the genes that encode identified proteins from the CC1 PUP-IT analyses were co-expressed with the *CESA* genes, we inspected their co-expression relationships. Here, we identified BFA-VISUALIZED ENDOCYTIC TRAFFICKING DEFECTIVE1 (BEN1)/ BREFELDIN A-INHIBITED GUANINE NUCLEOTIDE-EXCHANGE PROTEIN 5 (BIG5)/ *Arabidopsis thaliana* HopM interactor 7 (AtMIN7) as a promising candidate (Supplementary Fig. 4a; Supplementary Data 3, 4). In addition, several proteins previously reported to interact with BEN1, i.e. HYPERSENSITIVE TO LATRUNCULIN B1 (HLB1), Brefeldin A-inhibited guanine nucleotide-exchange protein 2 (BIG2) and *Arabidopsis thaliana* HopM interactor 10 (AtMIN10)[24], were also enriched in the Arabidopsis PafA-CC1 samples as compared to PafA-LTI6B (Fig. 2b). We therefore aimed to place BEN1 function in context of the CC1 and the CSC.

BEN1 is an ADP-ribosylation factor (ARF) guanine nucleotide exchange factor (ARF-GEF) involved in the trafficking of proteins between the TGN/Early Endosomes (EE) and the plasma membrane[25].

https://doi.org/10.1038/s41467-025-56192-3

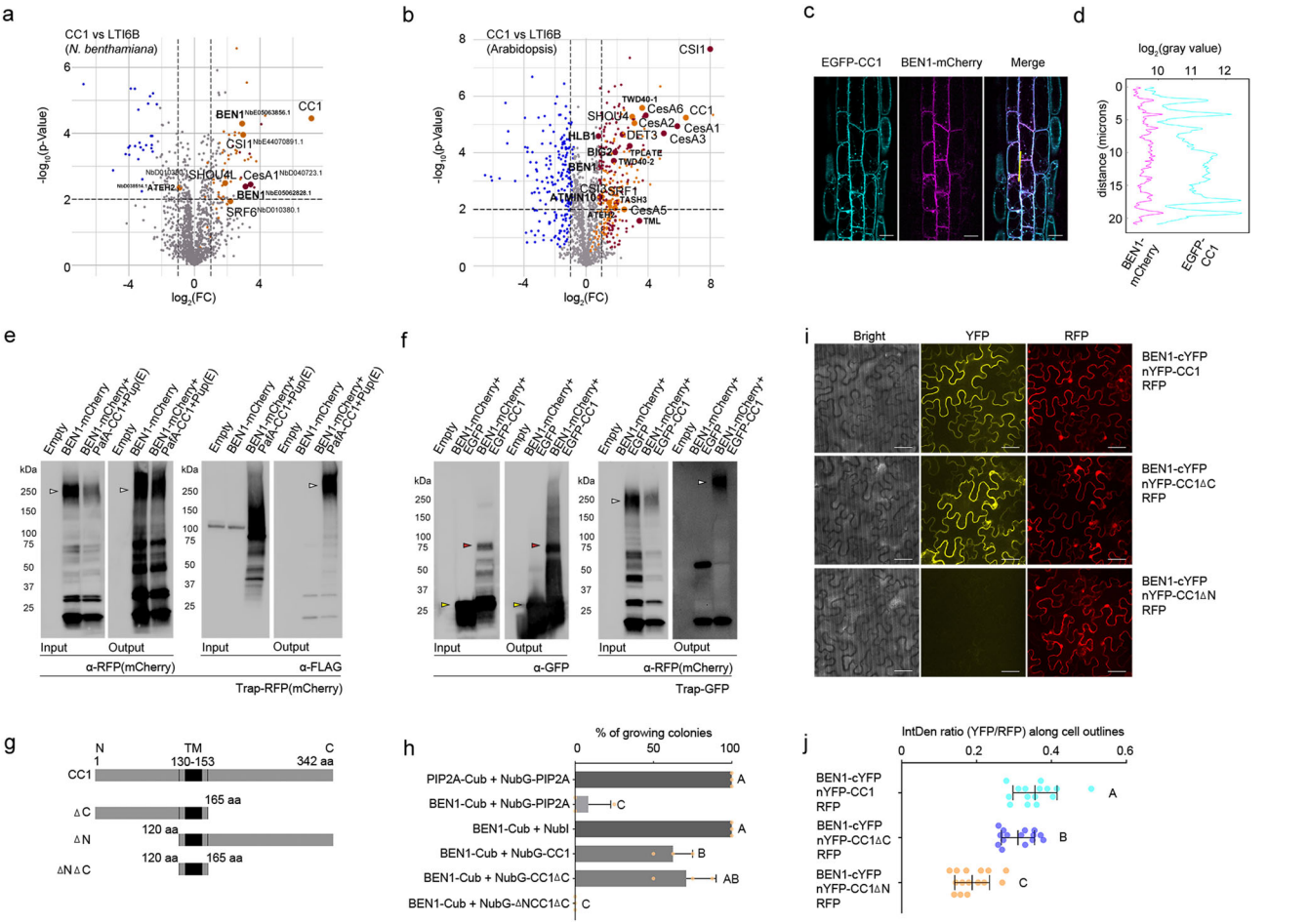

Fig. 2 | Employing PUP-IT to identify proteins in cellulose synthesis. a, **b** Volcano plots show differently enriched proteins in the PafA-CC1 and PafA-LTI6B groups from experiments in *N. benthamiana* (**a**) and Arabidopsis seedlings (**b**), based on a two-sided t-test with permutation-based FDR (FDR = 0.05, S0 = 1). Orange dots represent proteins unique to the PafA-CC1 group, maroon dots represent high-abundance proteins, gray dots represent proteins with no significant differences, and blue dots represent proteins more abundant in the control. CSC and BEN1-related proteins are marked with larger dots. **c** Co-localization of BEN1-mCherry and EGFP-CC1 in stable transgenic Arabidopsis. Scale bar = 10 μm. **d** Fluorescence intensity along the transect in (**c**). Images were taken from cells in the root tip area of 5-day-old seedlings. **e** BEN1-mCherry was labeled with FLAG when co-expressed with FLAG-Pup(E) and PafA-CC1 in *N. benthamiana*. RFP trap was used for immunoprecipitation, and α-RFP (mCherry) or α-FLAG antibodies for western blot. p19-only samples served as control. **f** BEN1-mCherry was co-immunoprecipitated with EGFP-CC1 in *N. benthamiana*. GFP trap was used for immunoprecipitation, and α-RFP (mCherry) or α-GFP antibodies for western blot. EGFP samples served as the negative control, and p19-only samples as the empty control. Arrowheads point to proteins of interest: BEN1-mCherry (white), EGFP (yellow) and EGFP-CC1 (red). **g** CC1 is a transmembrane protein with its N terminal facing the cytosol and C terminal in the apoplast, C terminal truncation (ΔC), N terminal truncation (ΔN). **h** Membrane split-ubiquitin Y2H was used to detect interactions between BEN1 and CC1, with CC1 constructs designed as shown in (**g**). Colony growth percentages on selection media from three replicates. Values are mean + SD. Significance was determined by one-way ANOVA followed by a Tukey's test ($p < 0.05$). **i** BiFC assay assessed the interaction between BEN1 and CC1, with CC1 constructs designed as shown in (**g**). Scale bar = 50 μm. **j** Relative YFP to RFP ratio was measured along the cell outlines in BiFC images. Values are mean ± SD. Significance was determined by one-way ANOVA followed by a Tukey's test ($p < 0.05$, $n = 15$).

To put the BEN1 localization in context to that of CC1, we co-expressed EGFP-CC1 and BEN1-mCherry in stable Arabidopsis lines and observed that the fluorescent signals co-localized at the plasma membrane and in endomembrane compartments (Fig. 2c, d; Supplementary Fig. 4b), in line with the function of both BEN1 and CC1 at the TGN[25,26]. These results indicated that the proteins may function at the same locations inside the cell. To confirm interactions between the two proteins, we first co-expressed BEN1-mCherry with the FLAG-Pup(E) and PafA-CC1 in *N. benthamiana*. These experiments showed that PafA-CC1 also could pupylate BEN1 in this transient infiltration system (Fig. 2e). To further corroborate interaction between BEN1 and CC1, we performed co-immunoprecipitation (co-IP) assays using *N. benthamiana* leaves. Here, we found that a EGFP-CC1 could co-IP BEN1-mCherry as compared to EGFP (Fig. 2f). To rule out that the BEN1-mCherry enrichment was due to the interaction to CC1 and not to spurious EGFP-mCherry interactions, we show that neither expression of EGFP nor EGFP-CC1 with mCherry revealed any co-IPed protein bands in the size region of BEN1-mCherry (Supplementary Fig. 4c). Interestingly, the molecular weight of the enriched BEN1-mCherry protein was substantially larger in the output of the co-IP experiment (Fig. 2f). One reason for this might be that the enriched BEN1-mCherry is poly-ubiquitinated, which has been reported for BEN1 in context of other PPIs[27]. Poly-ubiquitinated proteins may be targeted for degradation by the proteasome, which may be inhibited by applying the molecule MG132[28]. To assess whether the enriched BEN1-mCherry was poly-ubiquitinated, we therefore treated the samples with the proteasome inhibitor MG132 and probed the co-IPed BEN1-mCherry with an antibody that recognizes poly-Ubiquitin, with positive signal (Supplementary Fig. 4d). In addition, consistent with the notion that the poly-ubiquitinated BEN1-mCherry may be degraded, we also found that the treatment of MG132 led to an increased abundance of the poly-ubiquitinated BEN1-mCherry (Supplementary Fig. 4e).

We next further confirmed the interaction between BEN1 and CC1 using split-ubiquitin yeast two hybrid (Y2H) and *N. benthamiana*-based Bi-molecular Fluorescence Complementation (BiFC) assays. In the Y2H, we found that both CC1 and its C terminal truncation (fused to NubG) interacted weakly but consistently with BEN1 (fused to Cub). However, when we removed also the N-terminal region of CC1, we observed no interactions between the CC1 and BEN1 (Fig. 2g, h; Supplementary Fig. 4f). In the BiFC assays, we observed strong fluorescent signals when co-expressing nYFP-CC1 or nYFP-CC1ΔC with BEN1-cYFP, but detected only faint fluorescence when co-expressing nYFP-CC1ΔN and BEN1-cYFP (Fig. 2i). We quantified the fluorescence from the BiFC by including a 35S-driven RFP on the same backbone as the BiFC constructs, confirming our qualitative observations above (Fig. 2j). These results were not due to any mislocalization of the truncated versions of the CC1 as all the constructs still clearly labeled the plasma membrane (Fig. 2i, j; Supplementary Fig. 4g). From these analyses, we concluded that the N-terminal part of CC1 is necessary for the interaction of the protein with BEN1. The N-terminal part of CC1 consists of an intrinsically disordered region (IDR)[29]. Intriguingly, HopM1 (formerly hopPtoM) also interacts with BEN1 via its N terminus containing an IDR, which promotes poly-ubiquitination and degradation of BEN1[27]. Our results therefore highlight a related interaction mode and degradation scheme of BEN1 in relation to CC1 or HopM1. We speculate that CC1 and HopM1 either specifically recognize the poly-ubiquitinated BEN1, or recruits Ubiquitin ligase to BEN1 upon interaction, which in turn regulates the degradation of BEN1.

BEN1 regulates endomembrane trafficking of CC1 and the CSC

Given the general trafficking role of BEN1 at the TGN/EE, we next assessed how CC1 and BEN1 may functionally interact. We therefore grew *ben1* and *cc1cc2* mutant seedlings on media supplemented with the trafficking inhibitor BrefeldinA (BFA), a potent ARF-GEF inhibitor that leads to BFA-related endomembrane aggregates in the cytoplasm, also called BFA bodies[30]. Notably, *cc1cc2* mutant seedlings were more sensitive to the BFA conditions than wild type and showed similar defects in root elongation as that of the *ben1* mutant (Supplementary Fig. 5a, b)[31]. We next generated *ben1cc1cc2* triple mutants to investigate possible genetic interactions. Interestingly, *ben1cc1cc2* triple mutant plants displayed reduced rosette leaf expansion, which corresponded to a lower level of crystalline cellulose, as compared to wild-type (Fig. 3a, b; Supplementary Fig. 5c). In addition, *ben1cc1cc2* seedlings displayed increased sensitivity to the cellulose synthesis inhibitor isoxaben (Fig. 3c, d; Supplementary Fig. 5d).

We next sought to investigate the cell biological relationship between CC1 and BEN1. To do this, we attempted to directly visualize the dynamic behavior of CC1 and the CSC in the *ben1* mutant. We therefore introgressed Venus-CC1 and YFP-CESA6 into *ben1* plants. Previous studies showed that mutations in *BEN1* affect trafficking of, for example, PIN-FORMED (PIN) and BRASSINOSTEROID INSENSITIVE1 (BRI1), which led to reduced accumulation of the proteins in BFA bodies[25,32]. Consistent with these reports, we observed reduced accumulation of both Venus-CC1 and YFP-CESA6 in BFA bodies in the *ben1* mutant compared to the wild type (Fig. 3e, f). To investigate whether the BFA bodies were fueled from Endoplasmic Reticulum/Golgi (i.e. newly synthesized proteins en route to the TGN and plasma membrane), we pretreated seedlings with the de novo protein synthesis inhibitor cycloheximide (CHX), and then with BFA. These seedlings still contained substantial BFA bodies per cell (Fig. 3g; Supplementary Fig. 6a, b), indicating that BEN1 mainly is associated with trafficking of the CSC between the plasma membrane and the TGN/EE. To assess if the CSCs were unable to get to the plasma membrane, or if there were problems in CSC internalization, in the *ben1* mutant, we performed wash-out experiments of BFA. Here, the BFA bodies disappeared at similar rates in the *ben1* mutant and WT, indicating that BEN1 may be related to internalization of the CSCs and not CSC trafficking from the TGN to the plasma membrane (Supplementary Fig. 6a, b). Interestingly, the endocytosis of CSC is complex and may include both clathrin-dependent and independent processes[15]. To attempt to separate these processes in context of BEN1, we co-treated seedlings with the clathrin-mediated endocytosis inhibitor ES9-17 and CHX, and then with BFA. We found that this combination still led to BFA body formation, albeit to a substantially lesser degree than without ES9-17 (Fig. 3g, h; Supplementary Fig. 6c). These results highlight the clathrin-independent internalization of the CSCs, and indicate that BEN1 may contribute both to clathrin-dependent and -independent endocytosis of the CSC (Fig. 3g, h; Supplementary Fig. 6c). Finally, we checked YFP-CESA6 protein abundance and mRNA levels in *ben1* to see if the trafficking defects may also impact CESA6 levels. However, we did not find any major differences between *ben1* and WT control (Supplementary Fig. 6d, e). Taken together, our results indicate that BEN1 regulates the trafficking of the CSC between the plasma membrane and the TGN/EE and that defects in the BEN1 therefore impact cellulose synthesis.

Discussion

Protein interactions are essential to understand how proteins work in context to each other and to infer protein function. The implementation of new tools to study PPIs is therefore of substantial interest across all aspects of cell biology. We provide a new toolbox for PPI inferences, PUP-IT, in plant biology and highlight how this tool may be used to identify new components of important processes in plants.

We show that PUP-IT may be used in a range of different plant biological systems, including cell suspensions, transient infiltration assays and in stable transgenic plants. In addition, we supply several vector constructs where both the bait and the substrate can be included on a single backbone. The substrate may be modified with different tags to enrich the labeled proteins, which increases the versatility of the toolbox. It is, however, important to realize that the tag needs to be placed upstream of the PUP, as the PafA recognizes a phosphorylated PUP to then ligate onto Lysine residues on proteins close to the PafA[10,33]. We also compared PUP-IT against the highly popular TurboID. Here, we show that known interactors of TPLATE (used in the comparison as bait) were enriched to higher relative levels with PUP-IT as compared to TurboID and even against AP-MS. These results show that PUP-IT may have a higher specificity for close interactors, i.e. proteins forming protein complexes, than that of for example TurboID. We therefore envision that PUP-IT may become a preferred approach in the emerging field of protein proximity labeling.

Methods

Plant materials and growth conditions

T-DNA insertional lines for *ben1* (SALK_013761C) were obtained from NASC (http://Arabidopsis.info/); the double mutant *cc1cc2* (SAIL_838_F07, Gabi_654A12) and marker lines Venus-CC1 (*cc1cc2*), YFP-CESA6 (Col-0)[16] were as described in previous studies. *cc1cc2* was crossed to *ben1* to generate the triple mutant *cc1cc2ben1*, and plants *were* genotyped in the F2 generation. The fluorescent marker line YFP-CESA6 (Col-0) was crossed to *ben1*, with YFP-CESA6*ben1* identified via genotyping *ben1* and imaging of the YFP-CESA6. The fluorescent marker line Venus-CC1 (*cc1cc2*) was crossed to the triple mutant *cc1cc2ben1*, with Venus-CC1*cc1cc2ben1* identified via genotyping of *ben1* and imaging of Venus-CC1. The generated marker lines were re-examined in the F3 generation to confirm no segregations of the fluorescent markers and homozygosity of mutations. Primers used to screen homozygous insertion lines are present in Supplementary Table 1.

Arabidopsis seedlings were grown in a growth chamber under long-day conditions (16 h light/21 °C and 8 h dark/19 °C) on solid 1/2 Murashige and Skoog (MS) media with 1% sucrose for phenotyping. Seedlings from solid 1/2 MS media were transferred to soil pots in a greenhouse under conditions (16 h light/21 °C and 8 h dark/19 °C).

https://doi.org/10.1038/s41467-025-56192-3

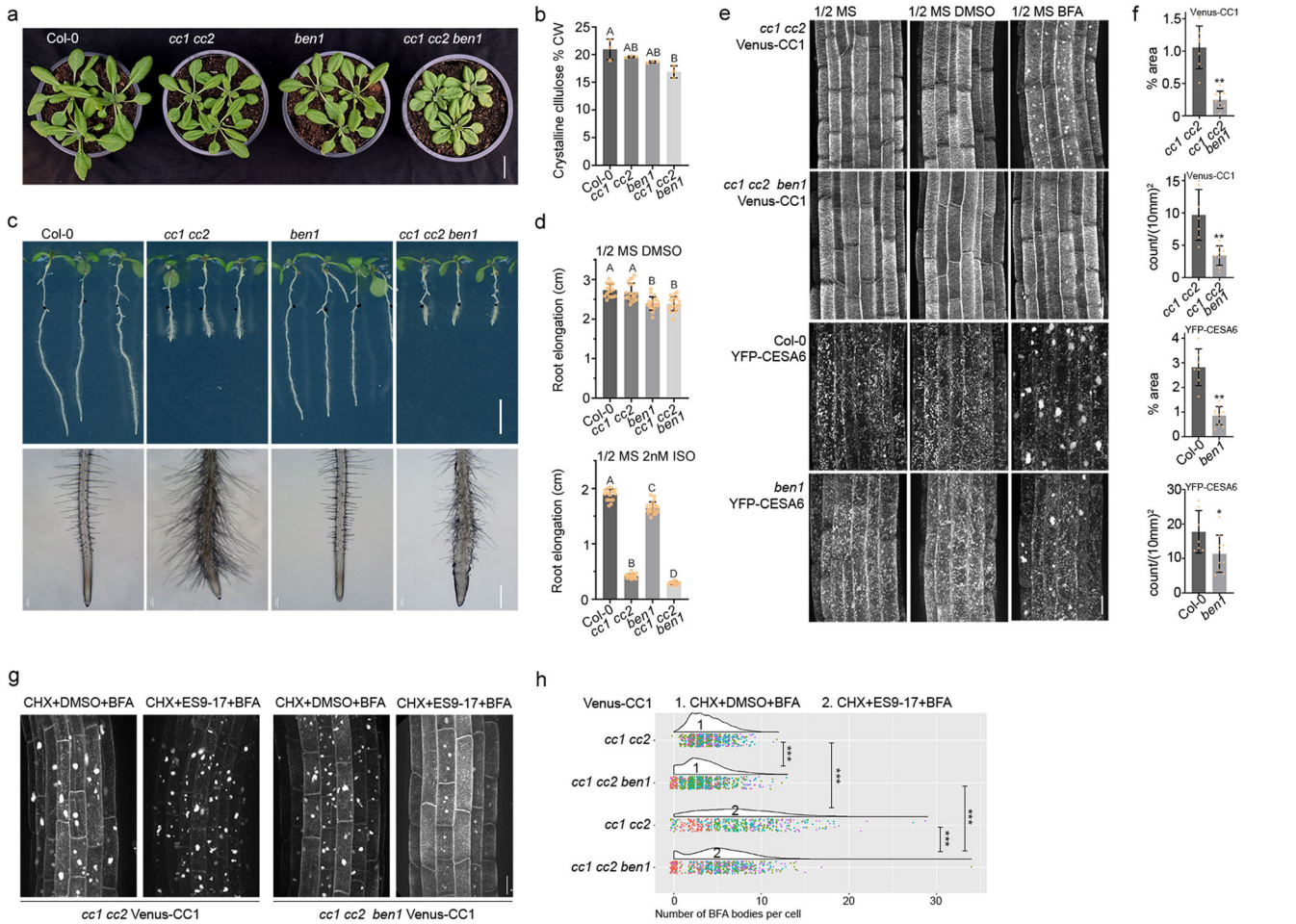

Fig. 3 | BEN1 impacts cellulose synthesis. a Five-day-old seedlings grown on 1/2 MS media were transferred to soil and grown for 18 days in the greenhouse. Scale bar = 2 cm. **b** Rosette leaves were harvested from plants as those in (**a**) and cellulose levels were measured. Values are mean ± SD. Significance was determined by one-way ANOVA followed by a Tukey's test ($p < 0.05$, $n = 3$). **c** Three-day-old seedlings grown on 1/2 MS media were transferred to media with 2 nM isoxaben for an additional 4 days. Scale bar = 0.5 cm (root elongation), scale bar = 0.5 mm (root tip area). **d** Root elongation after transfer to plates as indicated. Values are mean +/− SD. Significance was determined by one-way ANOVA followed by a Tukey's test ($p < 0.05$, $n \geq 15$). **e** Venus-CC1 and YFP-CESA6 in *ben1* or wild-type were imaged following BFA (50 μM for 30 min) or DMSO (control) treatments. Scale bar = 20 μm. **f** BFA body distribution across cells in the root area, percentage area (% area; upper panel) and count per mm² (lower panel) were used for statistical analyses. Values are mean±SD. Significance was determined by a two-sided t-test (* $p < 0.05$, ** $p < 0.01$, images from independent seedlings $n > 5$). **g** Venus-CC1 in *ben1* or wild-type backgrounds were imaged following CHX + ES9-17/DMSO + BFA treatment (CHX 50 μM for 60 min, followed by ES9-17 30 μM /DMSO for 30 min, then BFA 50 μM for 30 min.). Scale bar = 20 μm. **h** BFA body distribution was reflected by the number of BFA bodies per cell; ≥100 cells were counted from images of independent seedlings $n > 5$ for each experiment repeated four times. Data from each replicate is shown in a different color. Significance was determined by the Kruskal-Wallis test, followed by pairwise comparison using Wilcoxon test, *** $p < 0.001$.

Tobacco (*Nicotiana benthamiana*) used in this work were grown in the same conditions as above for 3 to 4 weeks.

Plasmid construction

Primers used for all the constructs in this manuscript and codon optimized sequence of PafA and Pup(E) are presented in Supplementary Table 1. Backbones and fragments were assembled with NEBuilder® HiFi DNA assembly mix (New England Biolabs)/In-fusion Master mix (Takara) or ligated using T4 ligase (Thermo Fisher Scientific/New England Biolabs) into corresponding cloning vectors.

To create the vectors that express the FLAG-Pup(E) and PafA fused proteins, fragments of FLAG-Pup(E) + ter3A were first assembled into the AscI site of pMDC32[34] to produce the destination vector pMDC32_35S::FLAG-Pup(E)::*ter3A*::*attR1-attR2*::*terNOS*. The UBI10 promoter and PafA were assembled into a pENTR vector. Then CDS of LTI6B and the pENTR backbone with *UBI10pro*::PafA were amplified and assembled. After that, an LR reaction was performed to integrate the linearized pENTR *UBI10pro*::PafA-LTI6B into the destination vector to produce the pMDC32_35S::FLAG-Pup(E)::*ter3A*_+_*UBIpro*::PafA-LTI6B::*terNOS*.

pENTR/TOPO with UBI10 promoter and multiple cloning sites was used as the backbone for the GFP/AtRACK1a/NbRACK1 vectors. pENTR/TOPO *CC1pro*::mNeonGreen-CC1::*terHSP* was used as the backbone for the CC1 vectors. HpaI or ApaLI (New England Biolabs) linearized pENTR of attL1-*UBIpro*::GFP/AtRACK1a/NbRACK1-PafA::-*terHSP*-attL2 and attL1-*UBIpro/CC1pro*::PafA-CC1::*terHSP*-attL2 were integrated into *pMDC32*_35S::FLAG-Pup(E)::*ter3A*::*attR1-attR2*::*terNOS*, respectively, through LR reactions.

To create the pGGK-35S::GRLhG4 > >A-G, vector pGG-A-35S-B, pGGD-linker-E, pGG-E-35St-F, pGG-F-AarI_linker-G[35] and the pSW610 (pGG-B-GR-LhG4-D[36]; addgene #115992) were assembled into a pGGK A-G vector via a Golden Gate reaction as previously described[35,37]. After AarI (Thermo Scientific™) digestion, an A-ccdB/CmR-G PCR fragment was inserted into the resulting vector via ligation using T4 DNA ligase to generate pGGK-35S::GRLhG4 > >A-ccdB-G. pGGK-35S::GRLhG4 > >p6xOP::StrepII-FLAG-PUP::*tHSP18.2*_+ _35S::TPLATE-

GSL-PafA.::*tHSP18.2* was created with two rounds of iterative Golden Gate assembly as previously described[37]. In the first Golden Gate reaction pGGK-35S::GRLhG4 > >A-ccdB-G was combined with pSW180a - pOp6 (pGG-A-p6xOP-B)[36], pGGB-StrepII-C, pGGC-FLAG-PUP-D, pGG-D-Decoy_v2-E (D017), pGG-E-tHSP18.2M-F[38] and pGG-F-A-AarI-SacB-AarI-G-G[35]. After AarI digestion, the resulting vector was combined with pGGA-35S-C[39], pGGC-TPLATE-D, pGGD-GSL-PafA-E, pGG-E-tHSP18.2M-F and pGG-F-linkerII-G[35] in a second Golden Gate reaction.

The CDS of *CC1* and *BEN1* (without stop codon) were amplified by PCR and subcloned into the entry vectors pUCL3L2 (Plasmid #114019, addgene) and pUCL1L4 (Plasmid #114018, addgene) respectively. Then pUCL1L4_BEN1 and pUCL3L2_CC1 were introduced into the pFRETgc-2in1-NC[40] (Plasmid #105121, addgene) vector by LR reaction to generate the pFRETgc_35S::EGFP_ + _35S::BEN1-mCherry and pFRETgc_35-S::EGFP-CC1_ + _35S::BEN1-mCherry. A pUCL1L4 with dummy sequence was generated to produce pFRETgc_35S::EGFP_ + _35S::mCherry and pFRETgc_35S::EGFP-CC1_ + _35S::mCherry.

The above-generated pUCL1L4_BEN1, pUCL3L2_CC1 and extra vectors with truncated CC1 in pUCL3L2 were introduced into the pBiFCt-2in1-NC[41] (Plasmid #1051112, addgene) and pFRETgc-2in1-NC to examine BiFC and protein subcellular localization signals.

The CDS of CC1, truncated CC1, PIP2A (without stop codon) and BEN1 (without stop codon) were subcloned in the pENTR/DTOPO and then introduced into the destination vectors pNX32-DEST (Plasmid #105083, addgene) and pMetYC-DEST (Plasmid ##105081, addgene) through LR reaction for split Y2H assay.

PUP-IT protein expression in *N. benthamiana*, *Arabidopsis thaliana* PSB-D cells and Arabidopsis plants

The Agrobacterium gv3101, transformed with either pMDC32_35S::FLAG-Pup(E)::*ter3A* _+_*UBIpro*::GFP/AtRACK1A/NbRACK1-PafA::*terHSP*, pMDC32_35S::FLAG-Pup(E)::*ter3A*_+_*UBIpro*::PafA-Lti6B::*terNOS*, or pMDC32_35S::FLAG-Pup(E)::*ter3A*_+_*UBIpro/CC1pro*::PafA-CC1::*terHSP*, was cultured and infiltrated into *N. benthamiana* leaves along with strain P19[42] (OD600 = 0.5 in infiltration buffer) as previously described[43]. The tissues were collected 2 days after plants were grown in the greenhouse.

The pGGK-35S::GRLhG4 > >p6xOP::StrepII-FLAG-PUP::*tHSP18.2*_ + _35S::TPLATE-GSL-PafA::*tHSP18.2* construct was transformed into dark grown PSB-D suspension culture cells as described before[44]. The cultures were harvested 3 days after subculturing. StrepII-FLAG-Pup(E) expression was induced with 1, 10, 50, 100 or 200 μM dexamethasone as indicated (stock solution: 50 mMol Dexamethasone in DMSO) for 1 or 24 h as indicated. DMSO was used as a mock treatment.

The Agrobacterium gv3101 transformed with either pMDC32_35S::FLAG-Pup(E)::*ter3A* _+_*UBIpro*::PafA-Lti6B::*terNOS* or pMDC32_35S::FLAG-Pup(E)::*ter3A*_+_ *CC1pro/UBIpro*::PafA-CC1::*terHSP* was used to produce Arabidopsis transgenics through floral dip method[45]. After hygromycin selection, positive transgenics were identified by western blot with FLAG antibody (see below). Seedlings were grown in liquid 1/2 MS media for six days in culture bottle to generate tissues for IP-MS.

SDS-PAGE and Western blot

Protein extractions from *N. benthamiana* leaves and Arabidopsis transgenics in 1× Laemmli loading buffer (BioRad) with reducing agent (100 mM DTT), were boiled for 10 min at 95 °C. Protein were loaded on a 12% or 4–15% SDS–PAGE TGX gel (BioRad) and subsequently blotted onto a polyvinylidenedifluoride membrane (BioRad). Membranes were blocked in 5% skimmed milk in TBST overnight at 4 °C on a shaking device. Next, the blots were incubated with primary antibodies α-FLAG (Merck, F3165, 1:2000), α-GFP (Chromotek, 3H9, 1:2000), α-YFP (Venus) (Merck, MABE1906, 1:1000) and secondary antibodies α-mouse-HRP (Agilent, P0260, 1:5000), α-rat-HRP (GE HealthCare, NA935V, 1:5000) in 5% skimmed milk for 1 h at room temperature on a shaking device. For RFP (mCherry) detection, membranes were blocked for 2 h at room temperature, incubated with primary antibody α-RFP (mCherry) (Chromotek, 6G6, 1:2000) overnight at 4 °C, and secondary antibody α-mouse-HRP (Agilent, P0260, 1:5000) for 1 h at room temperature on a shaking device. Same conditions for α-RFP were used for the α-Ubiquitin (Thermofisher, eBioP4D1, 1:500) western blots, with secondary antibody α-mouse-HRP (Agilent, P0260, 1:5000). Three times washes with 1 x TBST for 5 mins each were taken between the change of the primary antibody to the secondary antibody, and another three times washes for 5 mins each were taken before imaging the HRP signal under ChemiDoc.

Protein extractions from PSB-D suspension culture cells in 1× Laemmli loading buffer (BioRad) with reducing agent (1× NuPage [Invitrogen] or 100 mM DTT), were boiled for 10 min at 95 °C. Proteins were loaded on a 4–20% SDS–PAGE TGX gel (BioRad) and subsequently blotted on a polyvinylidenedifluoride membrane (BioRad). Membranes were blocked in 5% skimmed milk overnight at 4 °C on a shaking device. Next, the blots were incubated with primary antibodies α-FLAG (Merck, F1804, 1:1000], α-TPLATE[46](1:1000), α-AtEH1/Pan1[47](1:2000) and secondary antibodies α-mouse-HRP (Cytiva, NA931, 1:10,000), α-rabbit-HRP (Cytiva,NA934, 1:10,000) in 3% skimmed milk for 1 h at room temperature on a shaking device. Three times washes for 5 mins each were taken between the change of the primary antibody to the secondary antibody, and before imaging the HRP signal under ChemiDoc.

Protein extraction and immunoprecipitation

Tissues from *N. benthamiana* multiple leaves (2–3 g) were sampled and ground in liquid nitrogen to a fine powder. Total proteins were extracted with extraction lysis buffer (1:3 [W/V]- material: buffer), [20 mM Tris-HCl, pH 7.4, 150 mM NaCl, 5 mM $MgCl_2$, 1 mM EDTA, 1% Triton X-100, and 0.1% protease inhibitor cocktail (Roche)] for 30 min on ice, and centrifuged at 4 °C at 12,000 rpm for 30 min. The supernatant was divided into three equal amounts for the following independent immunoprecipitation triplicates, then incubated each with 100 μl equilibrated anti-Flag antibody coupled magnetic beads (Thermo Scientific™, A36797) for 2 h at 4 °C. Beads were washed three times with extraction buffer [20 mM Tris-HCl, pH 7.4, 150 mM NaCl, 5 mM $MgCl_2$, 1 mM EDTA, 1% Triton X-100 and 0.1% protease inhibitor cocktail (Roche)], then washed three times with wash buffer [20 mM Tris-HCl, pH 7.4, 150 mM NaCl, 5 mM $MgCl_2$, 1 mM EDTA and 0.1% protease inhibitor cocktail (Roche)] and three times with 1 X PBS. After that the beads were stored at −80 °C until LC-MS/MS analysis.

A similar process was performed on tissues from Arabidopsis seedlings (1–2 g) with three independent transgenic lines mixed. The extraction lysis buffer was replaced by [50 mM HEPES, pH 7.5, 150 mM NaCl, 10 mM NaF, 5 mM EDTA, 1% Triton X-100, 1% PVP and 0.1% protease inhibitor cocktail (Roche)], and the wash buffer was replaced by [50 mM HEPES, pH 7.5, 150 mM NaCl, 10 mM NaF, 5 mM EDTA, 1% PVP and 0.1% protease inhibitor cocktail (Roche)].

Total protein extracts from liquid N2 ground PSB-D cells (3 g/replicate) were generated by adding extraction buffer (2:3 - buffer:material), (25 mM TRIS-HCl pH7.6, 15 mM $MgCl_2$, 150 mM NaCl, 15 mM $pNO_2phenylPO_4$, 60 mM B-glycerophosphate, 0.1 mM Na_3VO_4, 1 mM NaF, 1 mM PMSF, 1 μm E64, 0.5 mM EDTA, 0.50% NP40, 5% ethyleneglycol, 0.1% protease inhibitor cocktail EDTA-free (Roche)]) and incubated for 1 h at 4 °C. Subsequently, the lysate was cleared by 2 centrifugation steps at 20,000 g at 4 °C. Then the lysate was incubated with equilibrated Strep-Tactin®XT 4Flow® high-capacity resin (100 μl beads/replicate) for 2 h at 4 °C. Next, the beads were washed 3 times (10 column volumes total). Bound proteins were eluted using either 2 × 50 μl 50 mM biotin [in 50 mM NH_4CO_3] or 2 × 50 μl 10% SDS [in 50 mM Triethylammonium bicarbonate (TEAB) pH 8.5]. Subsequently, the supernatant was cleared by 1-minute centrifugation at 20,000 g.

Protein samples eluted with SDS were cleaned up with S-Trap™ micro columns (Profiti). Protein samples eluted with biotin or SDS were digested in-solution with 1 μg Trypsin/LysC (Promega) overnight at 37 °C, followed with an additional 0.5 μg Trypsin/LysC for 2 h. Finally, digested proteins were cleaned up with C-18 Omix tips (Agilent). Digests containing the cleaved peptides were dried in a SpeedVac and stored at −20 °C until LC-MS/MS analysis.

Mass spectrometry and data analysis

Washed beads were incubated for 30 min with elution buffer 1 (2 M Urea, 50 mM Tris-HCl pH 7.5, 2 mM DTT, 20 μg/ml trypsin) followed by a second elution for 5 min with elution buffer 2 (2 M Urea, 50 mM Tris-HCl pH 7.5, 10 mM Chloroacetamide). Both eluates were combined and further incubated at room temperature overnight. Tryptic peptide mixtures were acidified to 1% TFA and loaded on Evotips (Evosep). Peptides were separated on 15 cm, 150 μM ID columns packed with C18 beads (1.9 μm) (Pepsep) on an Evosep ONE HPLC applying the '30 samples per day' method, and injected via a CaptiveSpray source and ten μm emitter into a timsTOF pro mass spectrometer (Bruker) ran in PASEF mode[48].

Peptides were re-dissolved in 20 μl loading solvent A (0.1% trifluoroacetic acid in water/acetonitrile (ACN) (98:2, v/v)) of which 2 μl was injected for LC-MS/MS analysis on an Ultimate 3,000 RSLCnano system in-line connected to a Q Exactive HF Biopharma mass spectrometer (Thermo). Trapping was performed at 20 μl/min for 2 min in loading solvent A on a 5 mm trapping column (Thermo scientific, 300 μm internal diameter (I.D.), 5 μm beads). 250 mm Aurora Ultimate, 1.7 μm C18, 75 μm inner diameter (Ionopticks) kept at a constant temperature of 45 °C. Peptides were eluted by a non-linear gradient starting at 1% MS solvent B reaching 26% MS solvent B (0.1% FA in acetonitrile) in 30 min, 44% MS solvent B in 38 min followed by a 5-minute wash at 56% MS solvent B starting at 40 min and re-equilibration with MS solvent A (0.1% FA in water) at a flow rate of 300 nl/min.

The mass spectrometer was operated in data-dependent mode and raw files were processed using the MaxQuant software (version 2.0.3.0)[49]. Peak lists were searched against the proteome of released *Nicotiana benthamiana*[50] or the proteome of Arabidopsis from Araport11plus database (www.arabidopsis.org/), combined with 262 common contaminants by the integrated Andromeda search engine. Additionally, the baits, PafA and FLAG-Pup(E) sequences were added. Mass tolerance on precursor ions was set to 4.5 ppm and on fragment ions to 20 ppm. Match between runs and MS1-based Label Free Quantification (LFQ) were on. The false discovery rate was 1% for both peptides (minimum length of 7 amino acids) and proteins.

The protein groups result file was uploaded in Perseus (version 2.0.3.0)[49]. Reverse hits, contaminants and only identified by site identifications were removed. LFQ intensity values were log2 transformed. For comparison between two groups, identifications were filtered for 50% values in total mimicking the assumption that specific proteins would be only detected in one group. A binary analysis was first performed to screen proteins as unique that were detected in all replicates within an experiment group but no detection in the corresponding control. For relative comparison, missing values were imputed with values around the detection limit, randomly drawn from a normal distribution with a width equal to 0.3 and a downshift equal to 1.8. Then a two-sided t-test was performed with false positive by permutation-based FDR calculation, using thresholds FDR = 0.05 and S0 = 1. For comparation of proteins from AtRACK1 and NbRACK1, an extra filter of $\log_2(FC) > 1$ was applied. The significant candidate lists were collected from proteins unique and relatively high abundance through t-test, then plotted in volcano summary by R.

Plant phenotyping

Seedlings of wild type (Col-0) and corresponding mutants were grown on 1/2 MS plates for 3 days, then transferred to the plates with 5 μM BFA for 7 days or 2 nM Isoxaben for 4 days (DMSO as control). The elongated root length was measured by FIJI-ImageJ, and the root tip were captured by KEYENCE (VHX-7000).

7-day-old seedlings were transferred into soil for 20 days in the greenhouse and pictured to record the growth of rosette leaves. 3 samples were harvested for each group, containing leaves from two pots. The crystalline cellulose quantification was conducted as described[51,52].

Immunoprecipitation, BiFC and split yeast two-hybrid assay

For FLAG-Pup(E) labeling assay, pFRETgc 35S.::EGFP_+_35S.::BEN1-mCherry were co-expressed with pMDC32_35S.::FLAG-Pup(E)_+_UBI-pro.::PafA-CC1 or not in *N. benthamiana* leaves, then proteins were immunoprecipitated by RFP-Trap Agarose (Chromotek, rta). For Co-IP, pFRETgc 35S.::EGFP_+_35S.::BEN1-mCherry, pFRETgc 35S.:: EGFP-CC1_+_35S.::BEN1-mCherry, pFRETgc 35S.::EGFP_+_35S.:: mCherry and pFRETgc 35S.::EGFP-CC1_+_35S.::mCherry were expressed in *N. benthamiana* leaves respectively, then proteins were immunoprecipitated by GFP-Trap Agarose (Chromotek, gta). The Immunoprecipitation was performed according to methods for Agarose Trap from Chromotek. Briefly, total proteins were extracted with buffer (1:3 [W/V]- material: buffer), [20 mM Tris-HCl, pH 7.4, 150 mM NaCl, 5 mM $MgCl_2$, 1 mM EDTA, 0.5% Triton X-100, and 0.1% protease inhibitor cocktail (Roche)] for 30 min on ice, and centrifuged at 4 °C at 12,000 rpm for 30 min. The supernatant was diluted with buffer [20 mM Tris-HCl, pH 7.4, 150 mM NaCl, 5 mM $MgCl_2$, 1 mM EDTA, and 0.1% protease inhibitor cocktail (Roche)], then incubated with 20 μl equilibrated RFP/GFP-Trap Agarose for 2 h at 4 °C. Beads were washed three times with buffer [20 mM Tris-HCl, pH 7.4, 150 mM NaCl, 5 mM $MgCl_2$, 1 mM EDTA, 0.05% Triton X-100 and 0.1% protease inhibitor cocktail (Roche)], After that, beads were boiled at 95 °C for 10 min with 1 × Laemmli loading buffer for western blot.

The pFRETgc-2in1-NC and pBiFCt-2in1-NC vectors with subcloned BEN1, CC1, or truncated CC1 were transformed into Agrobacterium gv3101. Transient expression in *N. benthamiana* and imaging were performed according to methods[40,41].

The split yeast two-hybrid assay was performed by employing an approach already developed[53]. Briefly, the tested group of plasmids were co-transformed into the yeast strain *NMY51*. The transformed yeast strains were plated on SD/-Leu/-Trp medium and placed in a 30 °C constant temperature incubator. For the interaction assay, colonies regrown on SD/-Leu/-Trp plate for three days were diluted in water and dropped on SD/-Leu/-Trp plate for 3 days, and on SD/-Leu/-Trp/-His/-Ade/-Met + 400 mM NaCl selection medium for 5–10 days to check growth. Experiments were repeated three times to evaluate survival ratios.

Drug treatments

Seedlings were grown on half MS plates vertically for 4–7 days. For BFA (Merck B6542-5MG or Sigma B7651-5MG) treatment, seedlings were placed in liquid 1/2 MS and treated with 50 μM BFA (stock solution 5 $mg.ml^{-1}$ in DMSO) or DMSO for 30/90 min under constant agitation before observation at the spinning microscope. For "BFA+washes", BFA treatment was followed by 3 washes of 20 min in half MS before observation.

In the case of cycloheximide treatment, seedlings in liquid 1/2 MS were pre-treated with 50 μM CHX (Sigma C7698-1G; stock solution 100 mM in DMSO) for 60 min before treatment with 50 μM CHX and 50 μM BFA for 90 min. Control seedlings were treated with 50 μM CHX for 150 min.

For clathrin-mediated endocytosis inhibition, seedlings in liquid 1/2 MS pre-treated with 50 μM CHX for 60 min were treated with Endosidin (Merck HY-131683 693806-53-0; stock solution 30 mM in DMSO) 30 μM or equivalent amount of DMSO for 30 min, followed by addition of 50 μM BFA for another 30 min.

Fluorescence imaging and analysis

Pictures were taken by Confocal Microscope 3i CSU-W SoRa Spinning Disk (Camera: Andor iXon Life 888 1024×1024 EMCCD) and processed by Fiji for image analyses. Cells from the elongation zone of the root from 5 to 7 days-old seedlings were used for imaging. The vector pFRETgc_35S::EGFP-CC1_+_35S::BEN1-mCherry was transformed into Col-0 and selected by BASTA for positive transgenics. Images were collected for EGFP (laser 488 nm, 30%, 100 ms) and mCherry (laser 561 nm, 30%, 200 ms), using a 100 X oil lens. For the mCherry bleach step, a defined region of interest was exposed to a bleach pulse through FRAP-Photoactivation unit (Vector2 VIS High-Speed Point Scanner) during a time-lapse imaging process. Lines were drawn across membranes to produce fluorescence intensity plots.

For BFA treatment, Venus-CC1 and YFP-CESA6 were excited by laser 514 nm (30%, 200 ms or 20%, 400 ms), and observed under a 60X oil lens with z-step of 0.3–1 μm. Number of BFA bodies per cell was quantified manually in Fiji using z-stacks of epidermal cells.

For imaging of *N. benthamiana* leaves, BiFC signals were collected of YFP (laser 514 nm, 20%, 200 ms) and RFP (laser 561 nm, 20%, 50 ms), using a 40 X air lens. For subcellular localization, fluorescence was collected of EGFP (laser 488 nm, 20%, 50 ms) and mCherry (laser 561 nm, 30%, 200 ms) using a 40X air lens.

YFP-CESA6 detection and q-PCR

Total proteins were extracted from 0.5 g seedlings of YFP-CESA6 marker lines in Col-0 and *ben1* background grown for 2 weeks on ½ MS plates. YFP-CESA6 were immunoprecipitated by GFP-Trap Agarose (Chromotek, gta) according to the method above, and detected by α-YFP (Venus) (Merck, MABE1906) in western blot.

Total RNA was extracted using plant total RNA kit (SIGMA, SLCD4163), cDNA was generated from iScript cDNA Synthesis Kit (BIO-RAD) and q-PCR (BIO-RAD, SYBR SYBR® Green qPCR mix) was performed according to the manufacturer's instructions with primers in Supplementary Table 1.

Statistics and Reproducibility

The statistics analysis was performed in GraphPad Prism (10), with all data available in the source data file. For representative results shown in the figures, conclusions were confirmed by repeated and coordinated experiments. The co-localization of BEN1-mCherry and EGFP-CC1 was observed from multiple transgenic lines with similar patterns. Co-IP of BEN1-mCherry and EGFP-CC1 were validated at least twice and supported by both positive results under conditions with MG132 treatment or not.

Accession numbers

PafA (Q8NQE1); Pup(E) (Q8NQE0); AtRACK1a (AT1G18080); TPLATE (AT3G01780); LTI6B(AT3G05890); CC1 (AT1G45688); CC2 (AT5G42860); BEN1 (AT3G43300); CESA6 (AT5G64740).

Reporting summary

Further information on research design is available in the Nature Portfolio Reporting Summary linked to this article.

Data availability

The Raw proteomics data generated in this study have been deposited in the PRIDE under accession code PXD048346. The processed source data is provided in the Supplementary Information/Source Data file. All material is available upon request to the corresponding author. Source data are provided with this paper.

References

1. Xing, S., Wallmeroth, N., Berendzen, K. W. & Grefen, C. Techniques for the analysis of protein-protein interactions in vivo. *Plant Physiol.* **171**, 727–758 (2016).
2. Bosch, J. A., Chen, C. L. & Perrimon, N. Proximity-dependent labeling methods for proteomic profiling in living cells: an update. *Wiley Interdiscip. Rev. Dev. Biol.* **10**, e392 (2021).
3. Yang, X. et al. Proximity labeling: an emerging tool for probing in planta molecular interactions. *Plant Commun.* **2**, 100137 (2021).
4. Liu, Q. et al. A proximity-tagging system to identify membrane protein-protein interactions. *Nat. Methods* **15**, 715–722 (2018).
5. Ye, R. Q. et al. Glucose-driven TOR-FIE-PRC2 signalling controls plant development. *Nature* **609**, 986 (2022).
6. Lin, Z. et al. Pupylation-based proximity-tagging of FERONIA-interacting proteins in Arabidopsis. *Mol. Cell Proteomics*, 100828 (2024).
7. Islas-Flores, T., Rahman, A., Ullah, H. & Villanueva, M. A. The receptor for activated C kinase in plant signaling: tale of a promiscuous little molecule. *Front Plant Sci.* **6**, 1090 (2015).
8. van Rosmalen, M., Krom, M. & Merkx, M. Tuning the flexibility of glycine-serine linkers to allow rational design of multidomain proteins. *Biochemistry* **56**, 6565–6574 (2017).
9. Jumper, J. et al. Highly accurate protein structure prediction with AlphaFold. *Nature* **596**, 583 (2021).
10. Ozcelik, D. et al. Structures of Pup ligase PafA and depupylase Dop from the prokaryotic ubiquitin-like modification pathway. *Nat. Commun.* **3**, 1014 (2012).
11. Ullah, H. et al. Structure of a signal transduction regulator, RACK1, from. *Protein Sci.* **17**, 1771–1780 (2008).
12. Gadeyne, A. et al. The TPLATE adaptor complex drives clathrin-mediated endocytosis in plants. *Cell* **156**, 691–704 (2014).
13. Arora, D. et al. Establishment of proximity-dependent biotinylation approaches in different plant model systems. *Plant Cell* **32**, 3388–3407 (2020).
14. Schwanhausser, B. et al. Global quantification of mammalian gene expression control. *Nature* **473**, 337–342 (2011).
15. Pedersen, G. B., Blaschek, L., Frandsen, K. E. H., Noack, L. C. & Persson, S. Cellulose synthesis in land plants. *Mol. Plant* **16**, 1228 (2023).
16. Endler, A. et al. A mechanism for sustained cellulose synthesis during salt stress. *Cell* **162**, 1353–1364 (2015).
17. Liu, Z. Y. et al. Cellulose-microtubule uncoupling proteins prevent lateral displacement of microtubules during cellulose synthesis in Arabidopsis. *Dev. Cell* **38**, 305–315 (2016).
18. Polko, J. K. et al. SHOU4 proteins regulate trafficking of cellulose synthase complexes to the plasma membrane. *Curr. Biol.* **28**, 3174–3182.e3176 (2018).
19. Chaudhary, A. et al. The Arabidopsis receptor kinase STRUBBELIG regulates the response to cellulose deficiency. *PLoS Genet.* **16**, (2020).
20. Lei, L., Li, S. D., Du, J., Bashline, L. & Gu, Y. Cellulose synthase interactive3 regulates cellulose biosynthesis in both a microtubule-dependent and microtubule-independent manner in Arabidopsis. *Plant Cell* **25**, 4912–4923 (2013).
21. Sanchez-Rodriguez, C. et al. The cellulose synthases are cargo of the TPLATE adaptor complex. *Mol. Plant* **11**, 346–349 (2018).
22. Luo, Y. et al. V-ATPase activity in the TGN/EE is required for exocytosis and recycling in. *Nature Plants* **1**, (2015).
23. Persson, S., Wei, H. R., Milne, J., Page, G. P. & Somerville, C. R. Identification of genes required for cellulose synthesis by regression analysis of public microarray data sets. *Proc. Natl. Acad. Sci. USA* **102**, 8633–8638 (2005).
24. Nomura, K., Imboden, L. A., Tanaka, H. & He, S. Y. Multiple host targets of Pseudomonas effector protein HopM1 form a protein complex regulating apoplastic immunity and water homeostasis. *bioRxiv*, (2023).
25. Tanaka, H., Kitakura, S., De Rycke, R., De Groodt, R. & Friml, J. Fluorescence imaging-based screen identifies ARF GEF component of early endosomal trafficking. *Curr. Biol.* **19**, 391–397 (2009).

26. Nomura, K. et al. Effector-triggered immunity blocks pathogen degradation of an immunity-associated vesicle traffic regulator in. *Proc. Natl. Acad. Sci. USA* **108**, 10774–10779 (2011).
27. Nomura, K. et al. A bacterial virulence protein suppresses host innate immunity to cause plant disease. *Science* **313**, 220–223 (2006).
28. Liu, L. et al. An efficient system to detect protein ubiquitination by agroinfiltration in Nicotiana benthamiana. *Plant J.* **61**, 893–903 (2010).
29. Kesten, C. et al. The companion of cellulose synthase 1 confers salt tolerance through a Tau-like mechanism in plants. *Nat. Commun.* **10**, (2019).
30. Chardin, P. & McCormick, F. Brefeldin A: The advantage of being uncompetitive. *Cell* **97**, 153–155 (1999).
31. Suo, Y. P. et al. BIG3 and BIG5 Redundantly Mediate Vesicle Trafficking in. *Biomolecules* **11**, (2021).
32. Xue, S. et al. Involvement of BIG5 and BIG3 in BRI1 Trafficking Reveals Diverse Functions of BIG-subfamily ARF-GEFs in Plant Growth and Gravitropism. *Int. J. Mol. Sci.* **20**, (2019).
33. Guth, E., Thommen, M. & Weber-Ban, E. Mycobacterial ubiquitin-like protein ligase PafA follows a two-step reaction pathway with a phosphorylated pup intermediate. *J. Biol. Chem.* **286**, 4412–4419 (2011).
34. Curtis, M. D. & Grossniklaus, U. A gateway cloning vector set for high-throughput functional analysis of genes in planta. *Plant Physiol.* **133**, 462–469 (2003).
35. Decaestecker, W. et al. CRISPR-TSKO: a technique for efficient mutagenesis in specific cell types, tissues, or organs in Arabidopsis. *Plant Cell* **31**, 2868–2887 (2019).
36. Schürholz, A. K. et al. A comprehensive toolkit for inducible, cell type-specific gene expression in Arabidopsis. *Plant Physiol.* **178**, 40–53 (2018).
37. Lampropoulos, A. et al. GreenGate - A Novel, Versatile, and Efficient Cloning System for Plant Transgenesis. *PLoS ONE* **8**, (2013).
38. Waadt, R., Krebs, M., Kudla, J. & Schumacher, K. Multiparameter imaging of calcium and abscisic acid and high-resolution quantitative calcium measurements using R-GECO1-mTurquoise in Arabidopsis. *N. Phytologist* **216**, 303–320 (2017).
39. Dragwidge, J. M. & Van Damme, D. Protein phase separation in plant membrane biology: more than just a compartmentalization strategy. *Plant Cell* **35**, 3162–3172 (2023).
40. Hecker, A. et al. Binary 2in1 Vectors Improve in Planta (Co)localization and Dynamic Protein Interaction Studies. *Plant Physiol.* **168**, 776–787 (2015).
41. Grefen, C. & Blatt, M. R. A 2in1 cloning system enables ratiometric bimolecular fluorescence complementation (rBiFC). *Biotechniques* **53**, 311–314 (2012).
42. Lakatos, L., Szittya, G., Silhavy, D. & Burgyán, J. Molecular mechanism of RNA silencing suppression mediated by p19 protein of tombusviruses. *Embo J.* **23**, 876–884 (2004).
43. Li, X. Y. et al. A distinct endosomal Ca/Mn pump affects root growth through the secretory process. *Plant Physiol.* **147**, 1675–1689 (2008).
44. Van Leene, J. et al. A tandem affinity purification-based technology platform to study the cell cycle interactome in. *Mol. Cell. Proteom.* **6**, 1226–1238 (2007).
45. Bechtold, N. & Pelletier, G. In planta Agrobacterium-mediated transformation of adult Arabidopsis thaliana plants by vacuum infiltration. *Methods Mol. Biol.* **82**, 259–266 (1998).
46. Dejonghe, W. et al. Disruption of endocytosis through chemical inhibition of clathrin heavy chain function. *Nat. Chem. Biol.* **15**, 641 (2019).
47. Grones, P. et al. The endocytic TPLATE complex internalizes ubiquitinated plasma membrane cargo (vol 8, pg 1467, 2022). *Nat. Plants* **9**, 191–191 (2023).
48. Meier, F. et al. Online Parallel Accumulation-Serial Fragmentation (PASEF) with a Novel Trapped Ion Mobility Mass Spectrometer. *Mol. Cell Proteom.* **17**, 2534–2545 (2018).
49. Tyanova, S., Temu, T. & Cox, J. The MaxQuant computational platform for mass spectrometry-based shotgun proteomics. *Nat. Protoc.* **11**, 2301–2319 (2016).
50. Kourelis, J. et al. A homology-guided, genome-based proteome for improved proteomics in the alloploid. *Bmc Genomics* **20**, (2019).
51. Updegraff, D. M. Semimicro determination of cellulose in biological materials. *Anal. Biochem* **32**, 420–424 (1969).
52. Kumar, M. & Turner, S. Protocol: a medium-throughput method for determination of cellulose content from single stem pieces of Arabidopsis thaliana. *Plant Methods* **11**, 46 (2015).
53. Grefen, C., Lalonde, S. & Obrdlik, P. Split-ubiquitin system for identifying protein-protein interactions in membrane and full-length proteins. *Curr. Protoc. Neurosci.* **Chapter 5**, Unit 5 27 (2007).

Acknowledgements

We acknowledge Prof Jürgen Kleine-Vehn for codon optimized templates of PafA and Pup(E). We would like to thank Liu Wang for sharing unpublished marker lines Venus-CC1*cc1cc2*. We thank Michael Kraus, Moritz Nowack, and Norbert Bollier for sharing unpublished golden gate building blocks. We thank Michaël Vandorpe for assisting with the golden gate cloning expression clones. We thank Geert De Jaeger and Jelle Van Leene for constructive discussions and the Interactomics Facility of the Center for Plant Systems Biology (VIB) for assisting with PSB-D cell culture transformation. We thank the Proteomics Research Infrastructure (PRI) at the University of Copenhagen (UCPH) supported by NNF19SA0059305 and the VIB proteomics core for the mass spectrometry data collection. We thank the Center for Advanced Bioimaging (CAB) at the UCPH for the imaging support. A.D.M. is supported by a PhD grant (1124621 N) from the Research Foundation– Flanders (FWO). L.C.N. is funded by EMBO ALTF 629-2021. G.A.K. is funded by a DECRA Fellowship from the Australian Research Council (DE210101200). S.P. was funded by a Villum, three Novo Nordisk, and Danish National Research Foundation grants (25915, 19OC0056076, 20OC0060564, 23OC0086341, DNRF155, respectively).

Author contributions

S.P. and S.Z. designed the experiments. S.Z. performed the major experiments. L.C.N. examined the protein trafficking under different conditions. O.K. provided help in generating transgenic plants and Western blots. G.A.K. produced the vector pMDC32_35S::FLAG-Pup(E)::ter3A::attR1-attR2::terNOS and pENTR UBI10pro::PafA-LTI6B. A.D.M., N.D.W., D.E., and D.v.D. tested the PUP-IT approach in Arabidopsis PSB-D suspension cells. S.Z. and S.P. wrote the manuscript. D.v.D. contributed to the writing.

Competing interests

The authors declare no competing interests.

Additional information

Supplementary information The online version contains supplementary material available at https://doi.org/10.1038/s41467-025-56192-3.

Correspondence and requests for materials should be addressed to Staffan Persson.

Peer review information *Nature Communications* thanks Yuanyuan Li and the other, anonymous, reviewers for their contribution to the peer review of this work. A peer review file is available.